

Entropy Production of the Willamowski-Rössler Oscillator

Jörg W. Stucki and Robert Urbanczik

Department of Pharmacology, University of Bern, Friedbühlstraße 49, CH-3010 Bern, Switzerland

Reprint requests to Prof. J. W. S.; Fax: +41 031 632 49 92; E-mail: Joerg.Stucki@pki.unibe.ch

Z. Naturforsch. **60a**, 599–607 (2005); received May 25, 2005

Some properties of the Willamowski-Rössler model are studied by numerical simulations. From the original equations a minimal version of the model is derived which also exhibits the characteristic properties of the original model. This minimal model shows that it contains the Volterra-Lotka oscillator as a core component. It thus belongs to a class of generalized Volterra-Lotka systems. It has two steady states, a saddle point, responsible for chaos, and a fixed point, dictating its dynamic behaviour. The chaotic attractor is located close to the surface of the basin of attraction of the saddle node. The mean values of the variables are equal to the (unstable) steady state values during oscillations even under chaos, and the variables are always non-negative as in other generalized Volterra-Lotka systems. Surprisingly this was also the case with the original reversible Willamowski-Rössler model allowing to compare the entropy production during oscillations with the entropy production of the steady states. During oscillations the entropy production was always lower even under chaos. Since under these circumstances less energy is dissipated to produce the same output, the oscillating system is more efficient than the non-oscillatory one.

Key words: Willamowski-Rössler Model; Entropy-production; Generalized Volterra-Lotka Systems; Mean and Steady State Values; Basins of Attraction.

1. Introduction

The Rössler oscillator was originally introduced as a particularly simple model, which showed chaotic behaviour, and surprisingly this needed only a quadratic nonlinearity [1]. For chemists, a major drawback of this model was that the variables could also assume negative values, and it was therefore not suited as a prototype of a chemical system exhibiting chaos. Later Willamowski and Rössler introduced another model, which was fully consistent with the basic requirements of chemical systems such as for example only positive values of the variables, detailed balance at equilibrium [2].

Surprisingly, only a few studies were dedicated to further investigate the special properties of this model. Aguda and Clarke, who identified the dynamic elements governing the behaviour of this oscillator and, in particular, suspected a similarity to the Volterra-Lotka (VL) model, thus far made the most detailed investigation [3]. Geysers and Nicolis applied the master equation to the Willamowski-Rössler (WR) model and established full consistency with thermodynamic principles [4].

In the present paper we investigate the entropy production of the model as well as the basin of attraction of the chaotic attractor. Furthermore, we will make a link between the WR model and the VL model by showing that the latter may serve as a core to the WR model.

2. The Willamowski-Rössler Model as Generalized Volterra-Lotka System

The differential equations of the original fully reversible WR model, considered as an open system containing the chemical species x , y and z as variables, read as follows [3]:

$$\begin{aligned}\dot{x} &= k_1x - k_{-1}x^2 - k_2xy + k_{-2}y^2 - k_4xz + k_{-4}, \\ \dot{y} &= k_2xy - k_{-2}y^2 - k_3y + k_{-3}, \\ \dot{z} &= -k_4xz + k_{-4} + k_5z - k_{-5}z^2.\end{aligned}\quad (1)$$

Already in their original paper Willamowski and Rössler noted that some of the rate constants could be set to very low values without much compromising the dynamics [2]. Indeed a minimal version of this model which still allows chaotic behaviour, consists in setting

the backward rate constants $k_{-2} = k_{-3} = k_{-4} = 0$ to obtain a minimal WR model (MWR):

$$\begin{aligned} \dot{x} &= k_1x - k_{-1}x^2 - k_2xy - k_4xz, \\ \dot{y} &= k_2xy - k_3y, \\ \dot{z} &= -k_4xz + k_5z - k_{-5}z^2. \end{aligned} \quad (2)$$

As shall be shown later, this case allows the analytical calculation of the steady states as a function of the rate constants k_i , which is not possible for the fully reversible model.

As a starting point of this study we will make a link between the MWR and the VL models since they seem to have interesting common mathematical structures. The differential equations of the celebrated VL model read

$$\begin{aligned} \dot{x} &= k_1x - k_2xy, \\ \dot{y} &= k_2xy - k_3y. \end{aligned} \quad (3)$$

The kinship between the two models is nicely seen by decomposing into independent components. The stoichiometry matrix for the MWR model can be written as

$$\mathbf{N} = \begin{pmatrix} 1 & -1 & 0 & -1 & 0 & -1 & 0 \\ 0 & 1 & -1 & 0 & 0 & 0 & 0 \\ 0 & 0 & 0 & -1 & 1 & 0 & -1 \end{pmatrix}, \quad (4)$$

where the rows stand for the variables x , y and z (downwards) and the columns for the forward reactions velocities (v_1, \dots, v_5) corresponding to the rate constants k_1, \dots, k_5 plus the two reverse reactions velocities (v_6, v_7), corresponding to k_{-1} and k_{-5} (from left to right). This system can be decomposed into independent components (or colors) by using the methods of chromokinetics [5]. This decomposition yields the following four basic colors:

$$\mathbf{colors} = \begin{pmatrix} 1 & 0 & 0 & 0 & 0 & 1 & 0 \\ 1 & 0 & 0 & 1 & 1 & 0 & 0 \\ 1 & 1 & 1 & 0 & 0 & 0 & 0 \\ 0 & 0 & 0 & 0 & 1 & 0 & 1 \end{pmatrix}, \quad (5)$$

where the columns follow the numbering scheme used for N and the four colors correspond to the rows of this matrix. We note that color 3 exactly corresponds to the Volterra-Lotka model. Figure 1 depicts a graphical interpretation of these four independent components of the minimal WR model. Color 2 has been called “switch” by Aguda and Clarke [3], whereas color 1 represents the autocatalytic reproduction of x ,

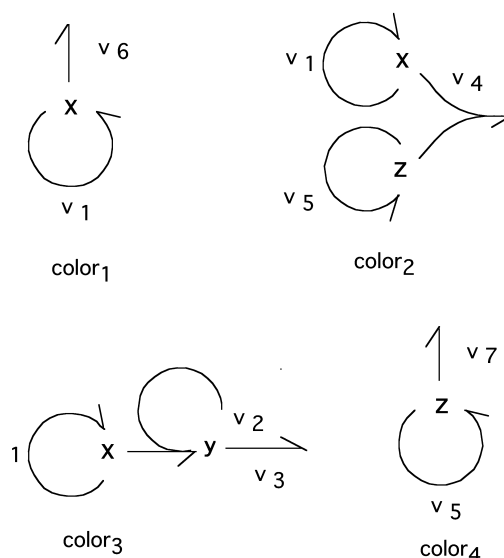


Fig. 1. Independent currents (basic colors) of the MWR. The color matrix (5) was graphically interpreted as partial reaction diagrams, each allowing an independent steady state with one degree of freedom. The steady state of the whole system is a convex combination of these basic colors. v_1 to v_7 correspond to the columns of the color matrix (5). In a steady state situation all v_i are identical in each diagram, whereas during oscillations they uncouple.

and color 4 the one of z . This representation again suggests a close similarity between the MWR and the VL model, and it seems that the VL component serves as a core in the WR model.

3. Basic Properties of Generalized Volterra-Lotka Systems

An n -dimensional generalization of the minimal WR model (2) is obtained by setting

$$\dot{x}_i = x_i(\mathbf{a}_i^T \mathbf{x} + b_i) + c_i \quad \text{for } i = 1, \dots, n, \quad (6)$$

where \mathbf{x} and the \mathbf{a}_i are n -dimensional vectors but the b_i as well as the c_i are scalars. We shall further assume that the c_i are non-negative.

This class of differential equations is a useful model of chemical reactions systems because the x_i remain non-negative if initially $\mathbf{x}(0) \geq 0$. This is easily seen in the following manner. Assume that, contrary to our claim, for some t we have $x_i(t) < 0$. Then $x_i(\tau) = 0$ must hold at some previous time $\tau < t$, since we have assumed $x_i(0) \geq 0$. Referring to (6), we see that $\dot{x}_i(\tau) = c_i \geq 0$, so the i -th component is either repelled ($c_i > 0$)

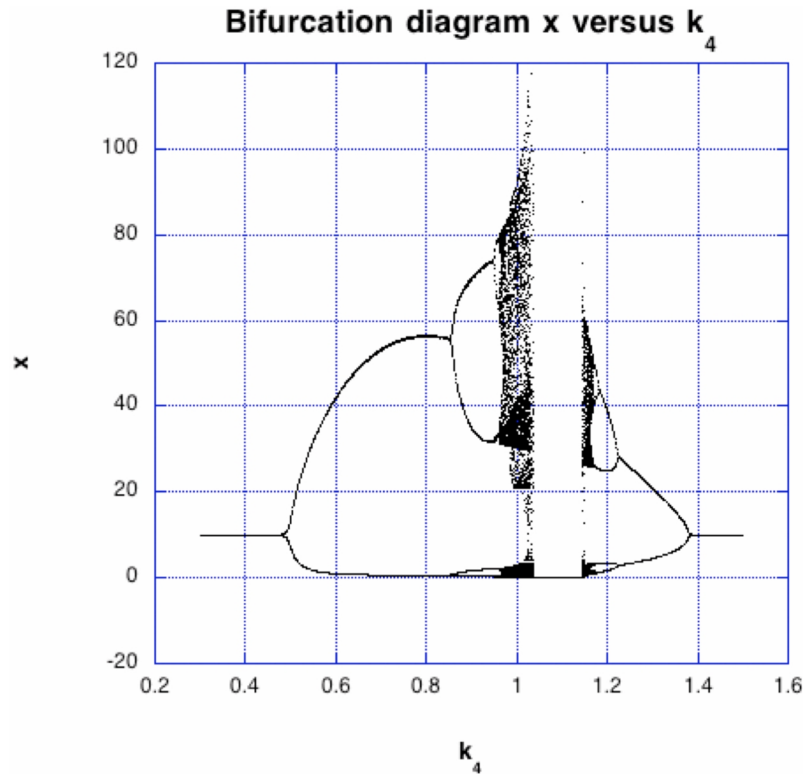


Fig. 2. Bifurcation diagram of the MWR. The following values of the rate constants were used: $k_1 = 30.0, k_2 = 1.0, k_3 = 10.0, k_5 = 16.5, k_{-1} = 0.25, k_{-5} = 0.5$. k_4 was varied from 0.3 to 1.5 in steps of 0.001. All other constants were set to zero. The initial conditions were $x(0) = y(0) = z(0) = 10.0$. The system (3) was numerically integrated for times 0 to 100. The points up to time 25 containing transients were discarded. From the remaining points, sampled in time intervals of 0.01, the inflection points of the time series were collected for the plot.

or stuck ($c_i = 0$) at the boundary and cannot cross into negative territory.

We now focus on the special case, analogous to the minimal WR model, that all the c_i are equal to zero. Then (6) has the rather remarkable property that the mean of x over the trajectory of the system is equal to one of the stationary points.

We first consider the stationary points of the system. Since $c_i = 0$, one of the factors in the first term of (6) must vanish at a stationary point x^s . We denote by Z the subset of indices for which the first factor x_i vanishes. Then x^s satisfies the n equations:

$$x_i^s = 0 \text{ for } i \in Z \text{ and } a_i^T x^s + b_i = 0 \text{ for } i \notin Z. \quad (7)$$

Note that (7) may not be solvable for all choices of Z . But if it is solvable for some Z , we have identified a stationary point.

Now we can show that under mild regularity conditions the mean over a trajectory is equal to one of the

stationary points. We fix one initial condition $x(0)$ and define the mean value by

$$\bar{x} = \lim_{t \rightarrow \infty} \frac{1}{t} \int_0^t x(\tau) d\tau. \quad (8)$$

For some indices i we may have $x_i(t)$ approaching 0 with increasing t , and we collect these indices into a set Z . We then also have

$$\bar{x}_i = 0 \text{ for } i \in Z. \quad (9)$$

For the remaining indices $i \notin Z$ we assume that the trajectory remains bounded and bounded away from zero, technically

$$0 < \varepsilon \leq x_i(t) \leq C \text{ for } i \notin Z \text{ and all } t \geq 0.$$

Then for $i \notin Z$ we can rewrite (6) as

$$\frac{\dot{x}_i}{x_i} = a_i^T x + b_i$$

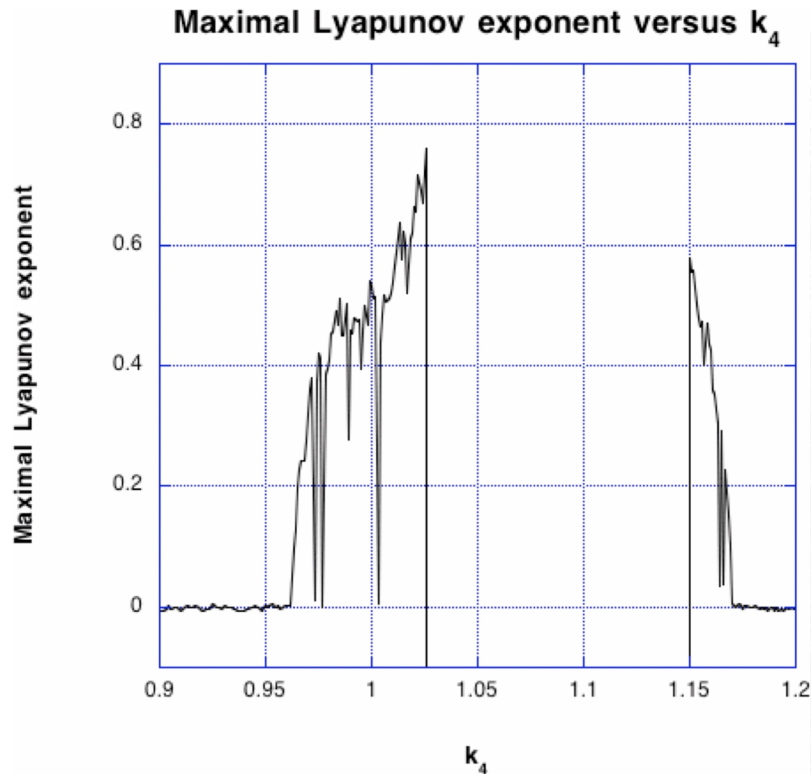


Fig. 3. Maximal Lyapunov exponents as a function of k_4 . All rate constants and initial conditions were as in Figure 2. k_4 was varied from 0.9 to 1.2 in steps of 0.001. Only the maximal Lyapunov exponents are shown. The two others were either zero or negative. Their sum was negative, indicating a dissipative system. The Lyapunov dimension reached a value of 2.08 (not shown).

and integrate to obtain $\ln x_i(t) = \mathbf{a}_i^T \int_0^t \mathbf{x}(\tau) d\tau + b_i t + c_i$. Dividing by t yields

$$\frac{\ln x_i(t)}{t} = \mathbf{a}_i^T \frac{1}{t} \int_0^t \mathbf{x}(\tau) d\tau + b_i + \frac{c_i}{t},$$

and sending $t \rightarrow \infty$

$$0 = \mathbf{a}_i^T \bar{\mathbf{x}} + b_i \text{ for } i \notin Z. \quad (10)$$

Now one sees that the conditions on $\bar{\mathbf{x}}$ (9) and (10) are identical to the ones for the stationary point (7).

3.1. Bifurcation Diagram and Lyapunov Exponents of the Minimal WR Model

In their publication Aguda and Clarke [3] noted that it is most convenient to study the dynamic properties of the WR model by using k_2 and k_4 as bifurcation parameters. Following this practice we integrated (2) by using a Runge-Kutta method contained in the IMSL library from Absoft together with their Fortran compiler (Version 7) on a Macintosh Cube computer. We noted

that the use of k_4 as a bifurcation parameter is superior to k_2 because it shows the whole range of bifurcations, whereas with k_2 the chaos disappears at $k_2 > 1.01$ and the system reaches a stable fixed point thereafter. A bifurcation diagram for the variation of k_4 is shown in Figure 2. This diagram demonstrates a period doubling route to chaos. Chaotic behaviour was also established by Aguda and Clarke on the basis of Shil'nikov's theorem [3]. For values of $k_4 > 1.025$, chaos disappears and the system settles to another stable steady state which is attractive already for $k_4 > 0.91$ since all its eigenvalues of the linearized system at steady state have negative real parts under these conditions (see below). Chaos reappears at $k_4 > 1.15$ and follows a period halving route to a stable steady state.

Moreover, the Lyapunov exponents were calculated [6] by again using k_4 as a bifurcation parameter. The graph depicted in Fig. 3 shows the maximal (positive) Lyapunov exponents, which clearly demonstrate chaos in the intervals $k_4 = (0.952, 1.025)$ and $k_4 = (1.15, 1.175)$.

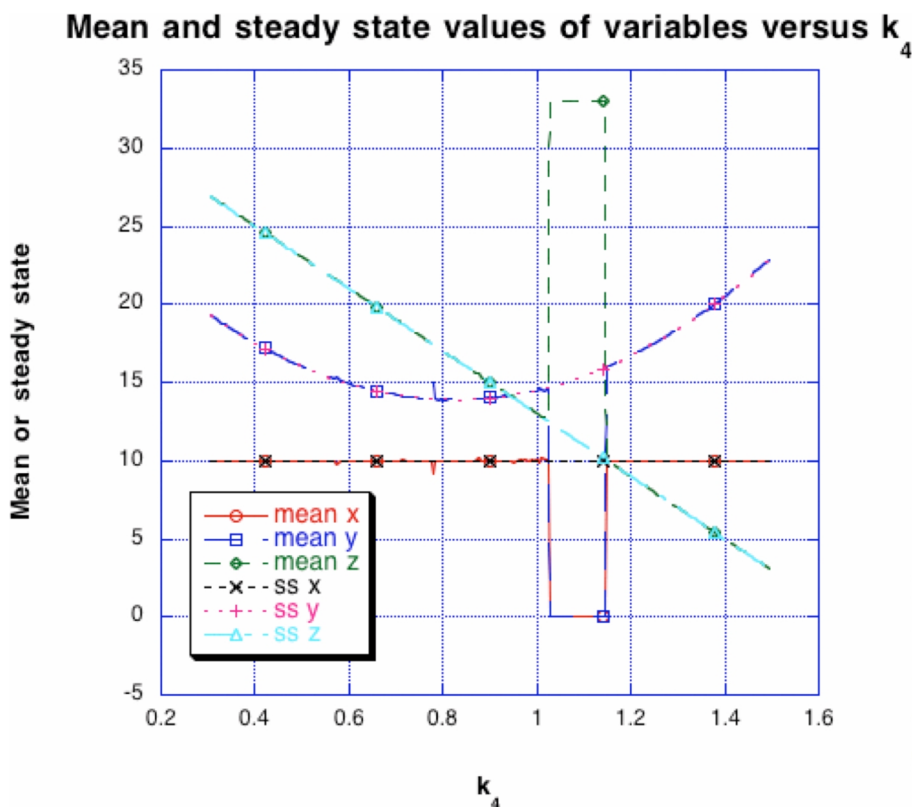


Fig. 4. Mean values of x , y and z during oscillations and non-oscillating steady states. For these calculations the full reversible WR model (1) was used. The rate constants and initial conditions were as in Fig. 1 and, in addition $k_2 = 0.0001$, $k_3 = k_4 = 0.001$. The steady states were calculated with an IMSL routine using the Jacobian matrix of the system. Except for the gap in the interval $k_4 = (1.025, 1.15)$, where the system settles at the fixed point (see text), the mean values and the steady state values were the same.

These calculations demonstrate that the minimal version of the WR model (2) is able to produce chaos. Further simplification of the model, viz. setting k_{-1} and k_{-5} also to zero, led to a fully irreversible system where chaos was no longer observed. This means that these two backward reactions are mandatory and in this sense (6) constitutes a minimal version of a WR model exhibiting chaotic behaviour. We will use this minimal version later to calculate the basins of attraction of the different steady states.

3.2. Mean Values and Entropy Production of the Willamowski-Rössler Oscillator

For the following calculations we again used the original fully reversible form of the WR model (1) and took k_4 as a bifurcation parameter, because this allowed to scan the full spectrum of dynamic behaviour

from a stable steady state to limit cycles and via period doubling to chaos, and then back again to a stable steady state.

In the numerical simulation shown in Fig. 4, we compare the mean values of the variables during oscillations with the numerically calculated values of the corresponding steady states. Of course during oscillations these steady states become unstable and act as repellors around which the system circulates. This is also corroborated by a linearized stability analysis which shows the transgression of the real parts of the eigenvalues through the imaginary axis into the positive part and then back again to negative real parts only by further increasing k_4 (not shown). Since the reverse of the rate constants k_3 and k_4 is very small, the mean values are equal to the steady states, as shown above for the minimal WR model. It must be stressed that in general the means do not correspond to the steady states during

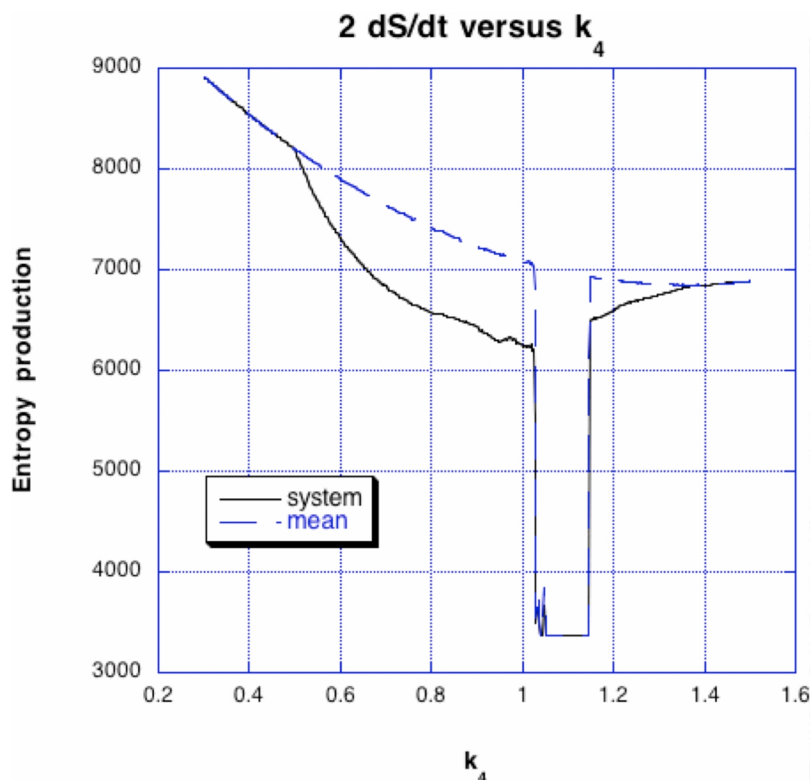


Fig. 5. Mean entropy production of the oscillations compared to that of the corresponding steady state. The same parameters as in Fig. 4 were used for the fully reversible WR model. Immediately after the onset of the limit cycle the entropy production of the oscillating system was always lower than for the non-oscillating system calculated from the mean values of the variables (corresponding to the steady state values). This plot demonstrates that oscillations lead to a diminished energy dissipation even under chaos.

oscillations. For example, in the original Rössler model the means are approximately twice as big as those in the steady states.

This exceptional behaviour allows to calculate the entropy production of the system for the values of the steady states, stable or not, and compare it to the entropy production of the system under oscillations. For the calculation of the entropy production (or the dissipation function) we proceeded as follows: The original WR model was split into two parts, one containing the forward reactions v (forward rate constants, k_{-i}) and one containing the reverse reactions v^{rev} (reverse rate constants, k_{-i}) giving the reaction velocities v and v_{rev} , respectively. From the definition of the classical chemical potential $1/T\mu_i = 1/T\mu_i^0 + \ln x_i$, where μ_i^0 is the standard chemical potential and x_i the concentration of the i -th species, and making use of the Gibbs relation between the entropy density S and the internal energy density, Clarke derived the following formula for the irreversible entropy production density from chemical

reactions (dissipation function) [7, pp. 95–96]

$$2\dot{S} = \sum_i (v_i - v_i^{\text{rev}}) \ln \frac{v_i}{v_i^{\text{rev}}}. \quad (11)$$

By splitting the reaction velocities of the WR model into forward and reverse reactions and by using (11), the mean entropy production was calculated for the parameter k_4 from 0.3 to 1.5 by sampling the points for v and v_{rev} in time intervals of 0.01 by integrating during 100 time units and after discarding the transients of the first 25 time units. Note that (11) corresponds to the conventional definition of the dissipation function $\sigma = \sum_i J_i X_i$, where $J_i = v_i - v_i^{\text{rev}}$ is the net flow and X_i the conjugate chemical force $A_i/RT = \ln v_i/v_i^{\text{rev}}$.

The diagrams depicted in Fig. 5 show that the entropy production drops to lower values as soon as there is an onset of the oscillations. This observation holds even for the system under chaos. Thus in this model less energy is dissipated during oscillations even though exactly the same output is produced. This can

be paraphrased by saying that the oscillatory system is more efficient than the non-oscillatory one. Unfortunately, however, the entropy production does not allow a classification of the dynamics of the system. There is clearly a drop of the entropy production, visible as soon as the Hopf bifurcation is reached and oscillations start. But finer details, such as period doubling or the onset of chaos, can not be deduced from the shape of the entropy production. In other words, entropy production is too coarse a measure for these transitions.

It is instructive to see how entropy production is distributed over the chaotic attractor or, in other words, where the “hot” and the “cold” regions are located. To illustrate this, we used the default lookup table of the T3D program from Fortner and colour coded the values of the entropy production in a 3D plot. Blue corresponds to low values of entropy production and red to the highest values. From that plot in Fig. 6 it can be deduced that the maximal dissipation is at the high x and y values near the ground plane, where the dynamics

mimics the VL oscillations. A histogram of the entropy production shows a sharp peak near the low values and a very flat distribution at higher values (not shown). Therefore the lowering of the entropy production is due to the fact that the trajectory density is highest at the origin characterized by low energy dissipation.

3.3. Basins of Attraction of the Minimal WR Model

From Fig. 5 it is apparent that variation of k_4 produced a gap between approximately 1 and 1.2. This was also observed in a more refined bifurcation diagram similar to the one in Fig. 2 (not shown). It was observed that upon increasing k_4 beyond 1, the z values were growing and reached a high stable steady state within the gap where chaos disappeared. This could be explained by a contact bifurcation driving the system into another stable steady state. An analysis revealed that the MWR model (3) has a total of 6 different steady states

$$\mathbf{ss} = \begin{bmatrix} 0 & 0 & 0 \\ \frac{k_1}{k_{-1}} & 0 & 0 \\ \frac{k_4 k_5 - k_1 k_{-5}}{k_4^2 - k_{-1} k_{-5}} & 0 & \frac{k_1 k_4 - k_{-1} k_5}{k_4^2 - k_{-1} k_{-5}} \\ \frac{k_3}{k_2} & \frac{k_1 k_2 - k_{-1} k_3}{k_2^2} & 0 \\ \frac{k_3}{k_2} & \frac{k_{-5} k_1 k_2 - k_{-1} k_{-5} k_3 + k_3 k_4^2 - k_2 k_4 k_5}{k_{-5} k_2^2} & \frac{k_2 k_5 - k_3 k_4}{k_{-5} k_2} \\ 0 & 0 & \frac{k_5}{k_{-5}} \end{bmatrix}. \tag{12}$$

We performed a local stability analysis by calculating the eigenvalues of the Jacobian as a function of k_4 , with the other parameters being as in Figure 2. This showed that \mathbf{ss}_5 is a saddle node in the range $0.5 < k_4 < 1.3$, with one negative real eigenvalue, and the other two eigenvalues forming a complex conjugate pair with positive real parts. The last \mathbf{ss}_6 is an attracting fixed point for $k_4 > 0.91$, since all the three eigenvalues have negative real parts in contrast to $k_4 < 0.91$, where at the minimum one of the eigenvalues has a positive real part. The dynamics of the system is dominated by these two steady states, and it depends on the initial values of the variables which steady state becomes relevant. To illustrate this, we calculated the dynamics of (6) for varying initial conditions at time zero for the variables x , y and z . This allowed to delineate the basins of attraction of the chaotic oscillator and

the stable steady state. The basin of attraction of the chaotic regime is depicted in Fig. 7 together with the chaotic attractor. It appears, that the attractor is located at the very surface of its basin of attraction. Within the transparent grey region chaos is attracting, and outside the fixed point becomes attractive. Thus it depends on the choice of the initial conditions whether the stable steady state becomes attractive or not. Note that in Fig. 7 the basins of attraction were only calculated for the standard set of rate constants as given in Figure 2. A perusal of different values of k_4 showed a rapid distortion and vanishing of the chaotic basin of attraction (not shown).

In summary, the dynamics of our MWR model is dictated by the two steady states \mathbf{ss}_5 and \mathbf{ss}_6 , one being a saddle node and the other a fixed point. In part this is also in accordance with the finding of others,

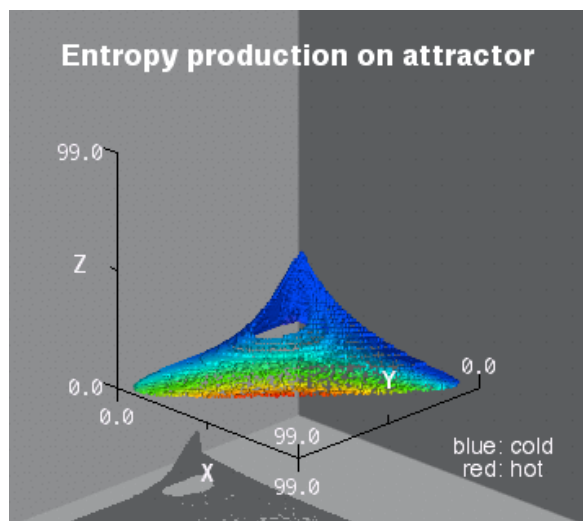


Fig. 6. Entropy production on the chaotic attractor. The values of the rate constants and initial conditions were chosen as in Fig. 5, and k_4 was set to 1. The values of the entropy production were color-coded using the LUT rainbow of the T3D program (see text). Blue regions correspond to low and red to high energy dissipation.

and in particular Aguda and Clarke proved chaos of the WR model with the help of Shil'nikov's theorem considering ss_5 [3].

4. Discussion

This study has shown that the MWR model (6) can be interpreted as an extension of the VL model. By contrast to the VL model which is conservative and has a constant of motion, our minimal model is dissipative and shows complex dynamics. There seems to be a large class of such autonomous systems (also called higher dimensional VL models). A prototype of such a generalized Volterra-Lotka system was published for example by Areneodo, Couillet and Tresser [8]. It also enjoys the properties of positive variables only and the means being equal to the (unstable) steady states. As shown above, this is one of the properties of generalized Volterra-Lotka systems.

Our main objective was to see whether an oscillating chemical system dissipates less energy than a non-oscillatory one. This comparison was possible due to the exceptional fact that the mean values of the oscillations were the same as the steady state values. Thus energy utilization for the production of the same amount of products in oscillating and non-oscillating modes could be compared. Clearly the oscillating system is

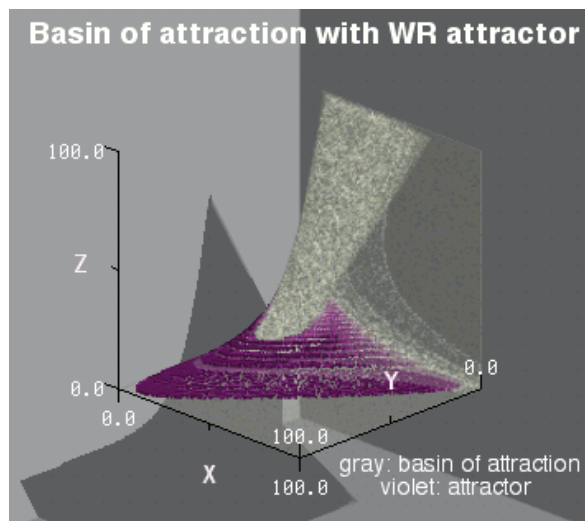


Fig. 7. Basins of attraction of the MWR with chaotic attractor. The values of the rate constants were as in Fig. 2 with $k_4 = 1.0$. The initial conditions of the variables x , y and z were varied from 0 to 100 in steps of 1. After integration during 50 time units and rejecting the transients it was decided whether the system oscillated around ss_5 (saddle node) or settled at ss_6 (fixed point). The basin of attraction of the chaotic trajectories is plotted in semitransparent gray with the embedded attractor depicted in opaque violet. In some regions of this basin of attraction the chaotic attractor lies close to the surface of the basin. All starting conditions of the variables outside this basin of attraction lead to the stable fixed point ss_6 (see text).

more efficient, and this might be useful for the design of synthetic methods in chemical plants in the industry. A study of the reversible Brusselator [9, 10] or Oregonator [11] also indicated a break to lower entropy production at the onset of oscillations, though a rigorous study is lacking.

The dynamics of the minimal WR model is dictated by two steady states, a saddle node and a fixed point, and each one has its basin of attraction for a fixed set of the rate constants. Different choices of the rate constants lead to different dynamics and basins of attraction. For example, increasing k_4 from 0.91 to higher values rapidly leads to a shrinking of the basin of attraction for the chaos. However, in this paper we refrained from scanning the parameter space much beyond the conventional values used in previous studies.

Another interesting question is whether or not spontaneous transitions between the chaotic attractor and the fixed point can ever occur. Thus far all numerical studies have shown, that this is not the case. This seems to be due to the number of particles involved.

For example, Geysermans and Nicolis used the master equation and showed that the chaotic attractor is resistant towards internal fluctuations in a moderately large system [4]. By contrast, in a study by Güémez and Matias [11], where a low number of particles was considered, integrations with the Gillespie [12] algorithm led to a rapid extinction of one of the species, suggesting sensitivity towards internal fluctuations. By perturbing this system with a special form of an external colored noise (a modified Langevin equation of diffusion) a transition between the two steady states (fixed point and chaos) could be realized. Thus we suspect, that resistance against internal fluctuations depends critically on the size of the system.

In summary, the WR model is a very interesting prototype of simple chemical models, which shows the whole palette of dynamics from stable steady states to limit cycles and chaos for a model obeying mass action kinetics. It would certainly be worthwhile to investigate similar models to gain more insight about oscillating chemical reactions and their energy requirements.

Acknowledgements

This study was supported by grants from the Swiss National Science Foundation. We are indebted to Dr. Clemens Wagner for helpful discussions.

- [1] O. E. Rössler, *Z. Naturforsch.* **31a**, 259 (1976).
- [2] K.-D. Willamowski and O. E. Rössler, *Z. Naturforsch.* **35a**, 317 (1980).
- [3] B. D. Aguda and B. Clarke, *J. Chem. Phys.* **89**, 7428 (1988).
- [4] P. Geysermans and G. Nicolis, *J. Chem. Phys.* **99**, 8964 (1993).
- [5] J. W. Stucki, *Eur. J. Biochem.* **271**, 2745 (2004).
- [6] J. Argyris, G. Faust, and M. Haase, *Die Erforschung des Chaos*, Vieweg, Braunschweig 1995.
- [7] B. Clarke, *Adv. Chem. Phys.* **43**, 1 (1980).
- [8] A. Areneodo, P. Couillet, and C. Tresser, *Phys. Lett.* **79a**, 259 (1980).
- [9] I. H. Lee, K.-Y. Kim, and U.-I. Cho, *Bull. Korean Chem. Soc.* **20**, 35 (1999).
- [10] A. K. Dutt, *J. Chem. Phys.* **86**, 3959 (1987).
- [11] J. Güémez and M. A. Matias, *Phys. Rev. E* **48**, 47 (1993).
- [12] D. T. Gillespie, *J. Phys. Chem.* **81**, 2340 (1977).